Bioorganic & Medicinal Chemistry 22 (2014) 1680–1689

Contents lists available at ScienceDirect

Bioorganic & Medicinal Chemistry

journal homepage: www.elsevier.com/locate/bmc

Synthesis of a novel series of thiazole-based histone acetyltransferase inhibitors

Daniela Secci [c], Simone Carradori [c], Bruna Bizzarri [c], Adriana Bolasco [c], Paola Ballario [b], Zoi Patramani [a], Paola Fragapane [a], Stefano Vernarecci [b], Claudia Canzonetta [b], Patrizia Filetici [a,*]

[a] Institute of Molecular Biology and Pathology, CNR, Sapienza University of Rome, P.le A. Moro 5, 00185 Rome, Italy
[b] Institute Pasteur-Fondazione Cenci Bolognetti, Department of Biology and Biotechnologies C. Darwin, Sapienza University of Rome, P.le A. Moro 5, 00185 Rome, Italy
[c] Department of Drug Chemistry and Technologies, Sapienza University of Rome, P.le A. Moro 5, 00185 Rome, Italy

ARTICLE INFO

Article history:
Received 20 September 2013
Revised 20 December 2013
Accepted 16 January 2014
Available online 26 January 2014

Keywords:
Histone acetyltransferase
Inhibitor
Acetylation
Thiazole
Gcn5
p300

ABSTRACT

Acetylation, which targets a broad range of histone and non-histone proteins, is a reversible mechanism and plays a critical role in eukaryotic genes activation/deactivation. Acetyltransferases are very well conserved through evolution. This allows the use of a simple model organism, such as budding yeast, for the study of their related processes and to discover specific inhibitors. Following a simple yeast-based chemogenetic approach, we have identified a novel HAT (histone acetyltransferase) inhibitor active both in vitro and in vivo. This new synthetic compound, 1-(4-(4-chlorophenyl)thiazol-2-yl)-2-(propan-2-ylidene)hydrazine, named BF**1**, showed substrate selectivity for histone H3 acetylation and inhibitory activity in vitro on recombinant HAT Gcn5 and p300. Finally, we tested BF**1** on human cells, HeLa as control and two aggressive cancer cell lines: a neuroblastoma from neuronal tissue and glioblastoma from brain tumour. Both global acetylation of histone H3 and specific acetylation at lysine 18 (H3AcK18) were lowered by BF**1** treatment. Collectively, our results show the efficacy of this novel HAT inhibitor and propose the utilization of BF**1** as a new, promising tool for future pharmacological studies.

1. Introduction

The genome architecture is a dynamic structure, which provides an actively regulated platform for gene expression influenced by different degree of compaction. Waves of chromatin remodeling allow transcription in response to external stimuli and environmental conditions. Centrally involved in this regulation is the chromatin structure whose accessibility is determined by nucleosome positioning which is affected by post-translational modifications (PTMs) such as acetylation, methylation, phosphorylation, ADP-ribosylation, and ubiquitination.[1] Chromatin modifiers deposit epigenetic PTMs on histone N-terminal tails or non-histone substrates and represent central pleiotropic regulators determining cell fate and differentiation.[2] Among other modifications, histone acetylation is a positive mark associated with active transcription that plays an important role in carcinogenesis and cancer therapy. Histone acetylation levels are finely regulated through a balanced competing activity of histone acetyltransferases (HATs) and histone deacetylases (HDACs). Interestingly, in tumor cells, either increasing or decreasing histone acetylation results in cell cycle arrest, redifferentiation and apoptosis.[3–5] Histone acetylation is catalyzed by Lys-acetyltransferases (KATs) grouped in five classes of enzymes conserved throughout evolution.[6] HATs and HDACs are centrally implicated in tumorigenesis by acting on oncogenes or oncosuppressors[2] and, accordingly, mutated forms have been found in several types of cancer. A growing number of examples where acetylation is involved in tumour etiology could be reported. It has been established that the pro-inflammatory NF-κB is involved in cellular transformation and it is well known the role of p300 as its coactivator; in addition recent studies revealed that NF-κB is also substrate of p300-mediated acetylation. It was demonstrated that curcumin—an acetyltransferase inhibitor of natural origin—is able to inhibit NF-κB and therefore to suppress proliferation.[7] Moreover, dysregulated Notch signaling, mainly upregulated by acetylation, is frequently observed in a variety of malignancies and consistently, HAT inhibitors are promising molecules for the pharmacological inhibition of this target.[8] Similarly, increased acetylation of STAT3 is found in tumors, such as breast cancer, therefore these observations provide a strong rationale for targeting HAT as a potential anticancer strategy.[9]

Along with the variety of pathological cellular states linked to the activity of certain members of the HAT family, we can include the Rubinstein–Taybi syndrome that is caused by specific

* Corresponding author. Tel.: +39 06 49912235.
E-mail address: patrizia.filetici@uniroma1.it (P. Filetici).

http://dx.doi.org/10.1016/j.bmc.2014.01.022
0968-0896/

chromosomal alterations corresponding to an area encoding for CBP. Other fusion proteins with aberrant histone acetyltransferase activity have been described as the main contributors to leukemogenesis. Moreover, increased p300 expression upon androgen starvation is crucial for prostate cancer cell proliferation,[10] clearly indicating the importance of targeting HATs in drug design.

Nevertheless, among the inhibitory molecules effective on chromatin modifiers, acetyltransferase inhibitors (HATi) described are fewer than the HDAC inhibitors.[11–13] Therefore, there is an active ongoing effort to identify specific modulators (activator/inhibitor) of HAT activity. Some already known active molecules are natural compounds extracted from plants such as curcumin,[14] anacardic acid,[15] garcinol and its synthetic derivatives,[16] epigallocatechin-3-gallate,[17] and plumbagin;[18] conversely, new and selective p300 inhibitors have been recently discovered by an extensive high-throughput screening program (*i.e.*, L002, C646).[19]

In addition, several authors have undertaken a series of studies involving the biological validation of new synthetic HATs inhibitors, with various degrees of selectivity and cell permeability. These can be divided into two different classes: the synthetic bisubstrate inhibitors (Lys-CoA, specific for p300, and H3-CoA-20, specific for PCAF)[20] and small molecules. Examples of this latest class are Gcn5 inhibitor butyrolactone MB-3,[21] a group of isothiazolones acting on p300/PCAF with anticancer properties in the micromolar range,[22–25] and different quinoline derivatives.[26,27]

In a previous study,[28] our lab identified the compound CPTH2 (Fig. 1A), from a series of cycloaliphatic thiazole-based derivatives, as a modulator of the HAT Gcn5 network. Accordingly, CPTH2 inhibited acetylation of recombinant Gcn5 in vitro and in vivo decreasing histone H3 global acetylation. Moreover, CPTH2 was used as an epigenetic modulator of essential functions in leukocytes.[29]

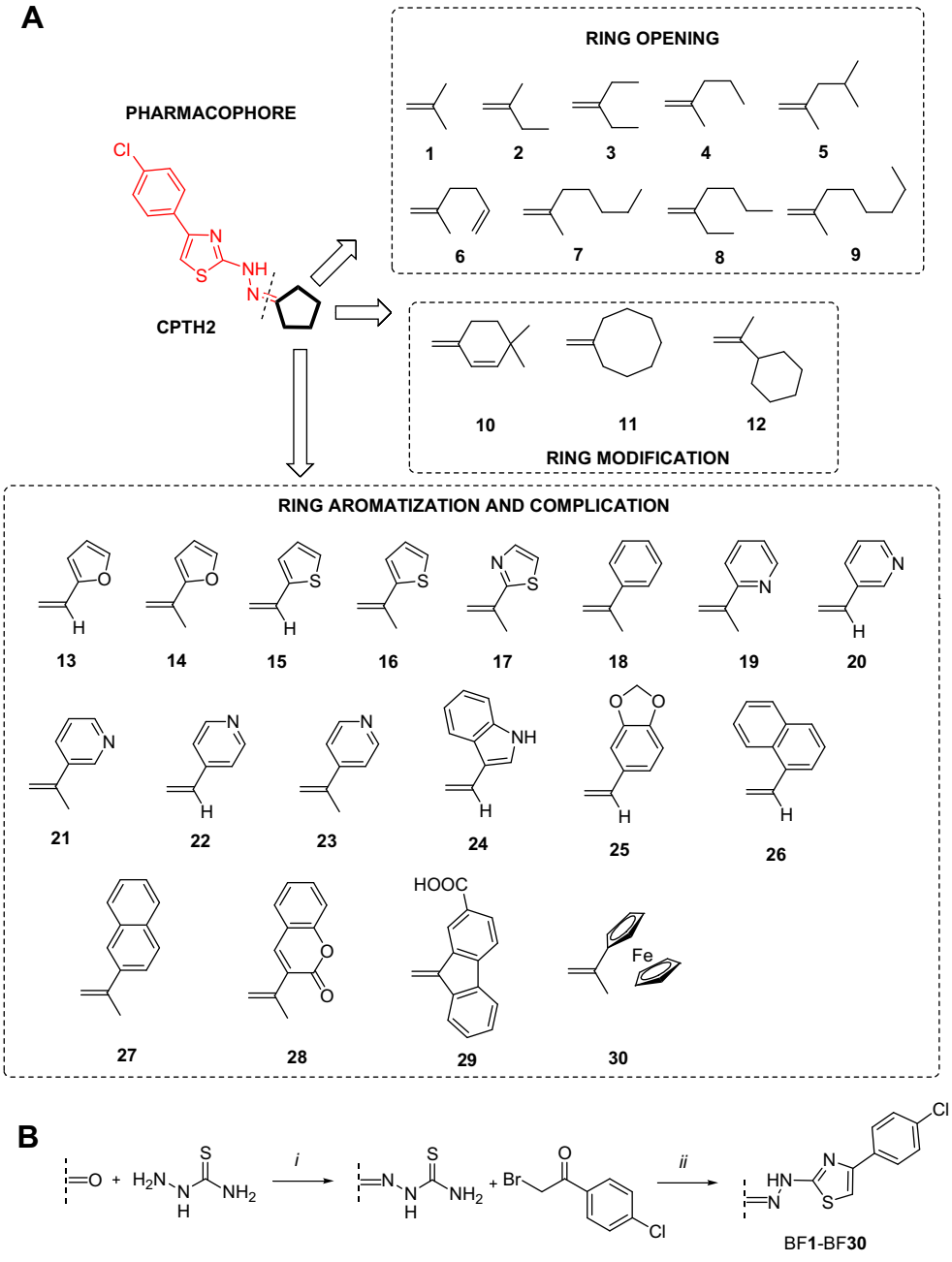

Figure 1. Lead modifications and general synthetic pattern. (A) Structural changes of the cyclopentane substituent on the hydrazonic nitrogen of the pharmacophore. (B) General synthetic pattern of BF**1**–BF**30** derivatives. Reagents and conditions: (i) acetic acid (cat.), EtOH; (ii) EtOH.

With the aim to identify compounds with specific HAT inhibitory activity, we developed novel molecules starting from this lead compound as shown in Figure 1. On the basis of HATs evolutionary conservation, we choose to screen in yeast *Saccharomyces cerevisiae* active compounds for their ability to inhibit growth of a strain deleted in GCN5. We based our screening on the genetic principle that deletion of two genes, whose function is connected, will produce a double mutant showing a sicker phenotype with respect to each single one. In line with this, we screened for compounds able to block a gene whose function is connected to our query gene, in this case GCN5 (Fig. 2). For this reason, we explored the effects of the chemical substitutions on the hydrazonic nitrogen with respect to the biological activity, by modifying the cyclopentane ring of the lead compound taking advantage of molecular simplification (ring opening, compounds BF**1**–BF**9**), cycle modification (BF**10**–BF**12**), and molecular complication (cycle aromatization, compounds BF**13**–BF**30**), without affecting the 4-(4-chlorophenyl)thiazol-2-ylhydrazine pharmacophore (Fig. 1A). Here we report on the synthesis of a large array of derivatives and the identification of a novel active compound, 1-(4-(4-chlorophenyl)thiazol-2-yl)-2-(propan-2-ylidene)hydrazine (BF**1**), derived from the lead compound CPTH2. The synthesized molecules were screened in yeast and compound BF**1**—which resulted active and selective on Gcn5 but not on other yeast HATs, such as Elp3,[30] Sas2,[31] and Rtt109[32,33]—was further characterized. The yeast methodology, with a simple and straightforward approach, allows the identification of synthetic molecules able to modulate key epigenetic regulatory hubs and to target genes involved in the functional response of a query gene, in this case HAT Gcn5. In addition, this assay may be employed in a variety of query deleted genes belonging to the same functional subgroup that is, acetyltransferases, methyltransferases, kinases etc. Finally, BF**1** was then tested in vitro for its activity on the catalytic Lys-acetylation reaction and its inhibitory activity was also confirmed in vivo against two aggressive tumour derived cell lines, glioblastoma-U87 and neuroblastoma-BE.

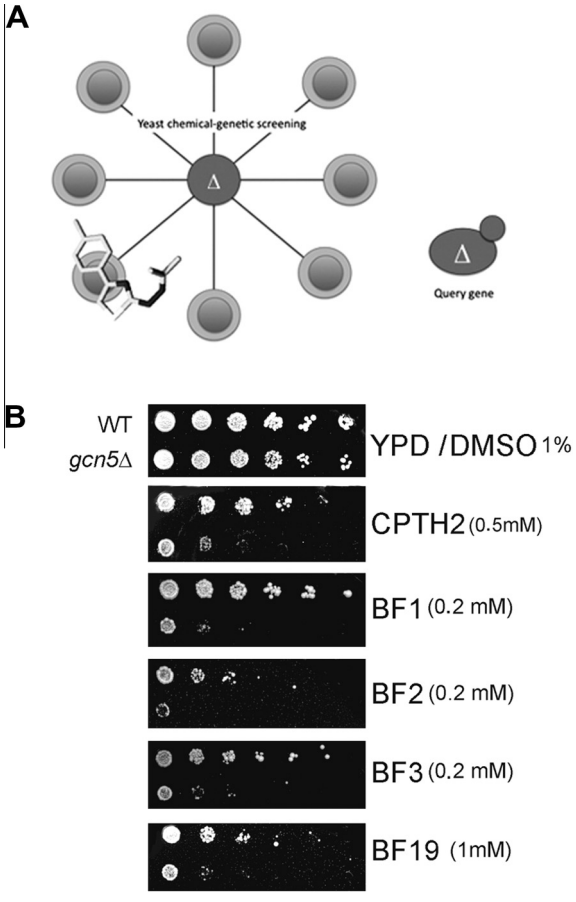

Figure 2. Screening in yeast *S. cerevisiae*. (A) Schematic representation of chemogenetic interaction in which small compounds can target a gene belonging to the functional network of the query gene. The result is a synthetic sick phenotype that resembles the phenotype produced by double deletions of interconnected genes. (B) Yeast growth spot assay. Liquid cell cultures were serially diluted (1/5), spotted on Petri dishes (solid medium) and grown for 48 h at 28 °C in presence of the compounds to be tested. The panel shows wild type (WT) and GCN5 deleted (*gcn5*Δ) strains grown in presence of the reported compounds, each dissolved in YPD/DMSO 1%. Presence of 1% DMSO itself is not toxic as shown in the first line of the panel.

2. Materials and methods

2.1. Chemistry

Starting materials and reagents were obtained from commercial suppliers and were used without further purification. Melting points (mp) were determined by the capillary method on an FP62 apparatus (Mettler-Toledo) and are uncorrected. ^{1}H NMR spectra were recorded at 400 MHz on a Bruker spectrometer using DMSO-d_6 or $CDCl_3$ as solvents. Chemical shifts are expressed as δ units (ppm) relative to TMS. Coupling constants J are expressed in hertz (Hz). Elemental analyses for C, H, and N were determined with a Perkin-Elmer 240 B microanalyzer and the analytical results were $\geqslant$95% purity for all compounds. All reactions were monitored by TLC on 0.2 mm thick silica gel plates (60 F_{254} Merck). Preparative flash column chromatography was carried out on silica gel (230–400 mesh, G60 Merck). Organic solutions were dried over anhydrous sodium sulfate. Concentration and evaporation of the solvent after reaction or extraction was carried out on a rotary evaporator (Büchi Rotavapor) operating at reduced pressure.

[4-(4-Chlorophenyl)thiazol-2-yl]hydrazine derivatives (BF**1**–BF**30**) were synthesized in high yields (83–99%) as reported in our previous studies.[34] Selected carbonyl compounds reacted directly with thiosemicarbazide in ethanol with catalytic amounts of acetic acid, and the obtained thiosemicarbazones were subsequently converted into (4-substituted-thiazol-2-yl)hydrazines by reaction with α,4-dichloroacetophenone in the same solvent (Hantzsch reaction) (Fig. 1B). All synthesized products were purified by washing with petroleum ether, hexane, and diethyl ether and by column chromatography (SiO_2, ethyl acetate/*n*-hexane) before characterization by ^{1}H NMR and elemental analysis.

Moreover, the presence of a C=N double bond can give rise to isomeric geometry *E*/*Z*. In some examples the ^{1}H NMR spectra analysis revealed that the *E* isomer was more favoured and stable than the *Z*-configuration by comparison of peaks area integration. Our choice, as reaction medium, of a polar alcoholic solvent appeared to be preferred to obtain the *E*-configuration and limit the interconversion according to the results of our previous theoretical and chromatographic study for similar compounds.[35]

2.2. General procedure for the synthesis of derivatives BF1–BF30

The appropriate carbonyl compound, aldehyde or ketone, (1.0 g, 50 mmol) was dissolved/suspended in 100 mL of ethanol and stirred with an equimolar quantity of thiosemicarbazide for 12–24 h at room temperature with catalytic amounts of acetic acid. Within 30 min the starting reaction mixture turned into a suspension and the precipitated thiosemicarbazone was filtered, washed with suitable solvent (petroleum ether, *n*-hexane, diethyl ether), and dried under vacuum. The structures of the synthesized intermediates were confirmed by ^{1}H NMR and TLC. Equimolar amounts of the prepared thiosemicarbazone (25 mmol) and α,4-dichloroacetophenone both suspended in ethanol, were reacted at room tempera-

ture under magnetic stirring for 12–24 h. The suspension was filtered on Gooch filter, washed with adequate solvents (diethyl ether, petroleum ether, hexane), and dried under vacuum. All products have been purified by column chromatography (SiO_2, ethyl acetate/*n*-hexane) to give compounds BF**1**–BF**30** in high yield.

2.3. Characterization data for new compounds

2.3.1. 1-(4-(4-Chlorophenyl)thiazol-2-yl)-2-(propan-2-ylidene)hydrazine (BF1)

White powder, 98% yield; mp 208–210 °C; ^{1}H NMR (DMSO-d_6) δ 2.10 (s, 3H, CH_3), 2.17 (s, 3H, CH_3), 6.72 (s, 1H, C_5H-thiazole), 7.50–7.52 (m, 2H, Ar), 7.70–7.72 (m, 2H, Ar), 12.35 (br s, 1H, NH, D_2O exch.). Anal. Calcd for $C_{12}H_{12}ClN_3S$: C, 54.23; H, 4.55; N, 15.81. Found C, 54.39; H, 4.69; N, 15.99.

2.3.2. 1-(Butan-2-ylidene)-2-(4-(4-chlorophenyl)thiazol-2-yl)hydrazine (BF2)

White powder, 89% yield; mp 203–205 °C; ^{1}H NMR (DMSO-d_6) δ 1.16–1.18 (m, 3H, CH_3), 2.20 (s, 3H, CH_3), 2.27–2.32 (m, 2H, CH_2), 6.70 (s, 1H, C_5H-thiazole), 7.26–7.27 (d, J = 8.1 Hz, 2H, Ar), 7.47–7.48 (d, J = 8.1 Hz, 2H, Ar), 12.38 (br s, 1H, NH, D_2O exch.). Anal. Calcd for $C_{13}H_{14}ClN_3S$: C, 55.81H, 5.04; N, 15.02. Found C, 55.50; H, 4.83; N, 15.30.

2.3.3. 1-(4-(4-Chlorophenyl)thiazol-2-yl)-2-(pentan-3-ylidene)hydrazine (BF3)

Grey powder, 85% yield; mp 177–179 °C; ^{1}H NMR (DMSO-d_6) δ 1,14–1,18 (m, 3H, CH_3), 1.23–1.27 (m, 3H, CH_3), 2.41–2.44 (m, 2H, CH_2), 2.54–2.57 (m, 2H, CH_2), 6.70 (s, 1H, C_5H-thiazole), 7.45–7.47 (d, J = 8.0 Hz, 2H, Ar), 7.66–7.68 (d, J = 8.0 Hz, 2H, Ar), 12.46 (br s, 1H, NH, D_2O exch.). Anal. Calcd for $C_{14}H_{16}ClN_3S$: C, 57.23; H, 5.49; N, 14.30. Found C, 57.01; H, 5.20; N, 14.59.

2.3.4. 1-(4-(4-Chlorophenyl)thiazol-2-yl)-2-(pentan-2-ylidene)hydrazine (BF4)

Grey powder, 83% yield; mp 207–209 °C; ^{1}H NMR (DMSO-d_6) δ 0.95–0.98 (m, 3H, CH_3), 1.60–1.64 (m, 4H, 2 × CH_2), 2.18 (s, 3H, CH_3), 7.27 (s, 1H, C_5H-thiazole), 7.46–7.48 (d, J = 7.9 Hz, 2H, Ar), 7.66–7.68 (d, J = 7.9 Hz, 2H, Ar), 12.45 (br s, 1H, NH, D_2O exch.). Anal. Calcd for $C_{14}H_{16}ClN_3S$: C, 57.23; H, 5.49; N, 14.30. Found C, 57.03; H, 5.17; N, 14.63.

2.3.5. 1-(4-(4-Chlorophenyl)thiazol-2-yl)-2-(4-methylpentan-2-ylidene)hydrazine (BF5)

Grey powder, 93% yield; mp 190–191 °C; ^{1}H NMR (DMSO-d_6) δ 0.95–0.96 (m, 6H, 2 × CH_3), 1.98–2.00 (m, 1H, CH), 2.18 (s, 3H, CH_3), 2.24–2.26 (m, 2H, CH_2), 6.69 (s, 1H, C_5H-thiazole), 7.46–7.48 (d, J = 7.8 Hz, 2H, Ar), 7.66–7.68 (d, J = 7.8 Hz, 2H, Ar), 12.39 (br s, 1H, NH, D_2O exch.). Anal. Calcd for $C_{15}H_{18}ClN_3S$: C, 58.52; H, 5.89; N, 13.65. Found C, 58.76; H, 5.60; N, 13.86.

2.3.6. 1-(4-(4-Chlorophenyl)thiazol-2-yl)-2-(hex-5-en-2-ylidene)hydrazine (BF6)

Green powder, 98% yield; mp 180–181 °C; ^{1}H NMR (DMSO-d_6) δ 2.19 (s, 3H, CH_3), 2.40–2.44 (m, 2H, CH_2), 2.50–2.55 (m, 2H, CH_2), 5.08–5.12 (m, 2H, =CH_2), 5.83–5.88 (m, 1H, =CH), 6.76 (s, 1H, C_5H-thiazole), 7.46–7.48 (d, J = 8.0 Hz, 2H, Ar), 7.66–7.68 (d, J = 8.0 Hz, 2H, Ar), 12.39 (br s, 1H, NH, D_2O exch.). Anal. Calcd for $C_{15}H_{16}ClN_3S$: C, 58.91; H, 5.27; N, 13.74. Found C, 59.23; H, 5.02; N, 14.02.

2.3.7. 1-(4-(4-Chlorophenyl)thiazol-2-yl)-2-(heptan-3-ylidene)hydrazine (BF7)

Grey powder, 86% yield; mp 171–173 °C; ^{1}H NMR (DMSO-d_6) δ 0.95–0.97 (m, 3H, CH_3), 1.15–1.18 (m, 3H, CH_3), 1.25–1.28 (m, 2H, CH_2), 1.48–1.51 (m, 2H, CH_2), 2.45–2.48 (m, 2H, CH_2), 2.53–2.56 (m, 2H, CH_2), 6.68 (s, 1H, C_5H-thiazole), 7.45–7.47 (d, J = 7.9 Hz, 2H, Ar), 7.67–7.69 (d, J = 7.9 Hz, 2H, Ar), 12.41 (br s, 1H, NH, D_2O exch.). Anal. Calcd for $C_{16}H_{20}ClN_3S$: C, 59.70; H, 6.26; N, 13.06. Found C, 59.56; H, 5.96; N, 13.44.

2.3.8. 1-(4-(4-Chlorophenyl)thiazol-2-yl)-2-(heptan-2-ylidene)hydrazine (BF8)

Grey powder, 89% yield; mp 158–160 °C; ^{1}H NMR (DMSO-d_6) δ 0.90–0.94 (m, 3H, CH_3), 1.33–1.35 (m, 4H, 2 × CH_2), 1.57–1.60 (m, 2H, CH_2), 2.10 (s, 3H, CH_3), 2.35–2.39 (m, 2H, CH_2), 6.60 (s, 1H, C_5H-thiazole), 7.46–7.48 (d, J = 8.0 Hz, 2H, Ar), 7.64–7.66 (d, J = 8.0 Hz, 2H, Ar), 12.48 (br s, 1H, NH, D_2O exch.). Anal. Calcd for $C_{16}H_{20}ClN_3S$: C, 59.70; H, 6.26; N, 13.06. Found C, 59.66; H, 5.99; N, 13.41.

2.3.9. 1-(4-(4-Chlorophenyl)thiazol-2-yl)-2-(octan-2-ylidene)hydrazine (BF9)

Grey powder, 97% yield; mp 163–165 °C; ^{1}H NMR (DMSO-d_6) δ 0.89–0.91 (m, 3H, CH_3), 1.25–1.29 (m, 4H, 2 × CH_2), 1.31–1.35 (m, 2H, CH_2), 1.57–1.59 (m, 2H, CH_2), 2.18 (s, 3H, CH_3), 2.36–2.39 (m, 2H, CH_2), 6.69 (s, 1H, C_5H-thiazole), 7.46–7.48 (d, J = 8.0 Hz, 2H, Ar), 7.64–7.66 (d, J = 8.0 Hz, 2H, Ar), 12.45 (br s, 1H, NH, D_2O exch.). Anal. Calcd for $C_{17}H_{22}ClN_3S$: C, 60.79; H, 6.60; N, 12.51. Found C, 61.12; H, 6.99; N, 12.89.

2.3.10. 1-(4-(4-Chlorophenyl)thiazol-2-yl)-2-(4,4-dimethylcyclohex-2-enylidene)hydrazine (BF10)

Light yellow powder, 97% yield; mp 230–233 °C; ^{1}H NMR (DMSO-d_6) δ 1.02 (s, 6H, 2 × CH_3), 1.58–1.59 (m, 2H, CH_2), 2.50–2.51 (m, 2H, CH_2), 5.96–5.99 (m, 2H, 2 × CH=), 7.33 (s, 1H, C_5H-thiazole), 7.43–7.45 (d, J = 7.9 Hz, 2H, Ar), 7.84–7.86 (d, J = 7.9 Hz, 2H, Ar), 12.41 (br s, 1H, NH, D_2O exch.). Anal. Calcd for $C_{17}H_{18}ClN_3S$: C, 61.53; H, 5.47; N, 12.66. Found C, 61.19; H, 5.88; N, 12.88.

2.3.11. 1-(4-(4-Chlorophenyl)thiazol-2-yl)-2-cyclooctylidenehydrazine (BF11)

Grey powder, 99% yield; mp 197–198 °C; ^{1}H NMR (DMSO-d_6) δ 1.44–1.46 (m, 2H, CH_2), 1.68–1.72 (m, 2H, CH_2), 1.89–1.95 (m, 3H, CH_2), 2.01–2.06 (m, 2H, CH_2), 2.46–2.51 (m, 3H, CH_2), 2.67–2.77 (m, 2H, CH_2), 6.69 (s, 1H, C_5H-thiazole), 7.45–7.48 (m, 2H, Ar), 7.66–7.69 (m, 2H, Ar), 12.39 (br s, 1H, NH, D_2O exch.). Anal. Calcd for $C_{17}H_{20}ClN_3S$: C, 61.15; H, 6.04; N, 12.59. Found C, 61.49; H, 5.88; N, 12.88.

2.3.12. 1-(4-(4-Chlorophenyl)thiazol-2-yl)-2-(1-cyclohexylethylidene)hydrazine (BF12)

Grey powder, 97% yield; mp 209–211 °C; ^{1}H NMR (DMSO-d_6) δ 1.30–1.35 (m, 6H, 3 × CH_2), 1.61–1.63 (m, 2H, CH_2), 1.70–1.72 (m, 1H, CH), 2.13–2.16 (m, 2H, CH_2), 2.18 (s, 3H, CH_3), 6.69 (s, 1H, C_5H-thiazole), 7.46–7.48 (d, J = 8.1 Hz, 2H, Ar), 7.66–7.68 (d, J = 8.1 Hz, 2H, Ar), 12.27 (br s, 1H, NH, D_2O exch.). Anal. Calcd for $C_{17}H_{20}ClN_3S$: C, 61.15; H, 6.04; N, 12.59. Found C, 61.50; H, 6.32; N, 12.27.

2.3.13. 1-(4-(4-Chlorophenyl)thiazol-2-yl)-2-(furan-2-ylmethylene)hydrazine (BF13)

Light brown powder, 98% yield; mp 225–227 °C; ^{1}H NMR (DMSO-d_6) δ 6.60–6.64 (m, 1H, furan), 6.80–6.82 (m, 1H, furan), 7.38 (s, 1H, C_5H-thiazole), 7.44–7.46 (d, J = 8.0 Hz, 2H, Ar), 7.79–7.81 (m, 1H, furan), 7.84–7.86 (d, J = 8.0 Hz, 2H, Ar), 7.91 (s, 1H, =CH), 12,24 (br s, 1H, NH, D_2O exch.). Anal. Calcd for $C_{14}H_{10}ClN_3OS$: C, 55.35; H, 3.32; N, 13.83. Found C, 55.54; H, 3.08; N, 13.48.

2.3.14. 1-(4-(4-Chlorophenyl)thiazol-2-yl)-2-(1-(furan-2-yl)ethylidene)hydrazine (BF14)

Yellow powder, 93% yield; mp 238–240 °C; ^{1}H NMR (DMSO-d_6) δ 2.22 (s, 3H, CH_3), 6.47–6.50 (m, 1H, furan), 6.87–6.89 (m, 1H,

furan), 7.45–7.47 (d, J = 7.9 Hz, 2H, Ar), 7.56 (s, 1H, C_5H-thiazole), 7.72 (m, 1H, furan), 7.87–7.89 (d, J = 7.9 Hz, 2H, Ar), 11.26 (br s, 1H, NH, D_2O exch.). Anal. Calcd for $C_{15}H_{12}ClN_3OS$: C, 56.69; H, 3.81; N, 13.22. Found C, 56.31; H, 3.49; N, 13.00.

2.3.15. 1-(4-(4-Chlorophenyl)thiazol-2-yl)-2-(thiophen-2-ylmethylene)hydrazine (BF15)

Grey powder, 97% yield; mp 230–231 °C; ^{1}H NMR (DMSO-d_6) δ 7.11–7.12 (m, 1H, tiophene), 7.35–7.36 (m, 1H, tiophene), 7.39–7.40 (m, 1H, tiophene), 7.44–7.46 (d, J = 8.0 Hz, 2H, Ar), 7.57 (s, 1H, C_5H-thiazole), 7.84–7.86 (d, J = 8.0 Hz, 2H, Ar), 8.22 (s, 1H, =CH), 12.44 (br s, 1H, NH, D_2O exch.). Anal. Calcd for $C_{14}H_{10}ClN_3S_2$: C, 52.57; H, 3.15; N, 13.14. Found C, 52.30; H, 3.40; N, 13.47.

2.3.16. 1-(4-(4-Chlorophenyl)thiazol-2-yl)-2-(1-(thiophen-2-yl)ethylidene)hydrazine (BF16)

Yellow powder, 88% yield; mp 245–247 °C; ^{1}H NMR (DMSO-d_6) δ 2.43 (s, 3H, CH_3), 7.07 (s, 1H, thiophene), 7.38 (s, 1H, thiophene), 7.44–7.46 (d, J = 8.0 Hz, 2H, Ar), 7.53 (s, 1H, C_5H-thiazole), 7.80–7.82 (d, J = 8.0 Hz, 2H, Ar), 7.85–7.88 (m, 1H, thiophene), 11.36 (br s, 1H, NH, D_2O exch.). Anal. Calcd for $C_{15}H_{12}ClN_3S_2$: C, 53.96; H, 3.62; N, 12.59. Found C, 54.19; H, 4.00; N, 12.28.

2.3.17. 1-(4-(4-Chlorophenyl)thiazol-2-yl)-2-(1-(thiazol-2-yl)ethylidene)hydrazine (BF17)

Light red powder, 86% yield; mp 230–231 °C; ^{1}H NMR (DMSO-d_6) δ 2.41 (s, 1H, CH_3), 7.45–7.47 (m, 2H, Ar), 7.57 (s, 1H, C_5H–thiazole), 7.68–7.70 (m, 2H, Ar), 7.73–7.75 (m, 1H, thiazole), 7.89 (m, 1H, thiazole), 11.33 (br s, 1H, NH, D_2O exch.). Anal. Calcd for $C_{14}H_{11}ClN_4S_2$: C, 50.22; H, 3.31; N, 16.73. Found C, 50.55; H, 3.02; N, 16.39.

2.3.18. 1-(4-(4-Chlorophenyl)thiazol-2-yl)-2-(1-phenylethylidene)hydrazine (BF18)

Light brown powder, 97% yield; mp 173–175 °C; ^{1}H NMR (DMSO-d_6) δ 2.34 (s, 3H, CH_3), 7.40–7.42 (m, 2H, Ar), 7.44–7.46 (d, J = 7.9 Hz, 2H, Ar), 7.53–7.55 (m, 2H, Ar), 7.58 (s, 1H, C_5H-thiazole), 7.63–7.65 (m, 1H, Ar), 7.87–7.89 (d, J = 7.9 Hz, 2H, Ar), 11.35 (br s, 1H, NH, D_2O exch.). Anal. Calcd for $C_{17}H_{14}ClN_3S$: C, 62.28; H, 4.30; N, 12.82. Found C, 62.01; H, 4.56; N, 13.07.

2.3.19. 1-(4-(4-Chlorophenyl)thiazol-2-yl)-2-(1-(pyridin-2-yl)ethylidene)hydrazine (BF19)

Dark yellow powder, 83% yield; mp 214–216 °C; ^{1}H NMR (DMSO-d_6) δ 2.40 (s, 3H, CH_3), 7.46 (s, 1H, C_5H-thiazole), 7.48–7.50 (m, 2H, Ar), 7.75–7.76 (m, 1H, pyridine), 7.86–7.88 (m, 2H, Ar), 8.10–8.12 (m, 1H, pyridine), 8.17–8.19 (m, 1H, pyridine), 8.89–8.91 (m, 1H, pyridine), 11.69 (br s, 1H, NH, D_2O exch). Anal. Calcd for $C_{16}H_{13}ClN_4S$: C, 58.44; H, 3.98; N, 17.04. Found C, 58.10; H, 4.29; N, 17.31.

2.3.20. 1-(4-(4-Chlorophenyl)thiazol-2-yl)-2-(pyridin-3-ylmethylene)hydrazine (BF20)

Yellow powder, 96% yield; mp 245–249 °C; ^{1}H NMR (DMSO-d_6) δ 7.46–7.48 (m, 2H, Ar), 7.49 (s, 1H, C_5H-thiazole), 7.86–7.88 (m, 2H, Ar), 7.90 (s, 1H, =CH), 8.13–8.15 (m, 1H, pyridine), 8.50–8.56 (m, 1H, pyridine), 8.60–8.63 (m, 1H, pyridine), 9.00 (s, 1H, pyridine), 12.59 (br s, 1H, NH, D2O exch.). Anal. Calcd for $C_{15}H_{11}ClN_4S$: C, 57.23; H, 3.52; N, 17.80. Found C, 57.54; H, 3.09; N, 17.49.

2.3.21. 1-(4-(4-Chlorophenyl)thiazol-2-yl)-2-(1-(pyridin-3-yl)ethylidene)hydrazine (BF21)

Yellow powder, 85% yield; mp 235–236 °C; ^{1}H NMR (DMSO-d_6) δ 2.38 (s, 3H, CH_3), 7.46 (s, 1H, C_5H-thiazole), 7.48–7.50 (d, J = 8.7, 2H, Ar), 7.77–7.79 (m, 1H, pyridine), 7.88–7.90 (d, J = 8.7 Hz, 2H, Ar), 8.51–8.53 (m, 1H, pyridine), 8.70–8.71 (m, 1H, pyridine), 9.02 (s, 1H, pyridine), 11.65 (br s, 1H, NH, D_2O exch). Anal. Calcd for $C_{16}H_{13}ClN_4S$: C, 58.44; H, 3.98; N, 17.04. Found C, 58.05; H, 4.26; N, 17.37.

2.3.22. 1-(4-(4-Chlorophenyl)thiazol-2-yl)-2-(pyridin-4-ylmethylene)hydrazine (BF22)

Orange powder, 94% yield; mp 278–280 °C; ^{1}H NMR (DMSO-d_6) δ 7.47–7.49 (d, J = 8.0 Hz, 2H, Ar), 7.58 (s, 1H, C_5H-thiazole), 7.86–7.88 (d, J = 8.0 Hz, 2H, Ar), 8.05–8.07 (m, 2H, pyridine), 8.12 (s, 1H, =CH), 8.79–8.81 (m, 2H, pyridine), 13.38 (br s, 1H, NH, D_2O exch.). Anal. Calcd for $C_{15}H_{11}ClN_4S$: C, 57.23%; H, 3.52; N, 17.80. Found C, 57.61; H, 3.12; N, 18.03.

2.3.23. 1-(4-(4-Chlorophenyl)thiazol-2-yl)-2-(1-(pyridin-4-yl)ethylidene)hydrazine (BF23)

Red powder, 86% yield; mp >280 °C; ^{1}H NMR (DMSO-d_6) δ 2.38 (s, 3H, CH_3), 7.48–7.50 (m, 2H, Ar), 7.56 (s, 1H, C_5H-thiazole), 7.89–7.91 (m, 2H, Ar), 8.14–8.16 (m, 2H, pyridine), 8.81–8.83 (m, 2H, pyridine), 12.04 (br s, 1H, NH, D_2O exch). Anal. Calcd for $C_{16}H_{13}ClN_4S$: C, 58.44; H, 3.98; N, 17.04. Found C, 58.69; H, 4.19; N, 17.36.

2.3.24. 1-((1*H*-Indol-3-yl)methylene)-2-(4-(4-chlorophenyl)thiazol-2-yl)hydrazine (BF24)

Grey powder, 98% yield; mp 222–224 °C; ^{1}H NMR (DMSO-d_6) δ 7.18–7.21 (m, 2H, indole), 7.33 (s, 1H, C_5H-thiazole), 7.43–7.46 (m, 2H, indole), 7.76 (s, 1H, =CH), 7.86–7.88 (d, J = 8.0 Hz, 2H, Ar), 8.21 (s, 1H, indole), 8.23–8.25 (d, J = 8.0 Hz, 2H, Ar), 11.50 (br s, 1H, NH-indole, D_2O exch.), 11.89 (br s, 1H, NH, D_2O exch.). Anal. Calcd for $C_{18}H_{13}ClN_4S$: C, 61.27; H, 3.71; N, 15.88. Found C, 61.59; H, 3.45; N, 16.09.

2.3.25. 1-(Benzodioxol-5-ylmethylene)-2-(4-(4-chlorophenyl)thiazol-2-yl)hydrazine (BF25)

Yellow powder, 83% yield; mp 240–242 °C; ^{1}H NMR (DMSO-d_6) δ 6.06 (s, 2H, CH_2, benzodioxole), 6.97–6.98 (m, 1H, benzodioxole), 7.21–7.22 (m, 1H, benzodioxole), 7.37 (s, 1H, C_5H-thiazole), 7.44 (s, 1H, =CH), 7.45–7.47 (d, J = 7.8 Hz, 2H, Ar), 7.85–7.87 (d, J = 7.8 Hz, 2H, Ar), 7.94–7.95 (m, 1H, benzodioxole), 12.65 (br s, 1H, NH, D_2O exch.). Anal. Calcd for $C_{17}H_{12}ClN_3O_2S$: C, 57.06; H, 3.38; N, 11.74. Found C, 57.39; H, 3.65; N, 11.50.

2.3.26. 1-(4-(4-Chlorophenyl)thiazol-2-yl)-2-(naphthalen-1-ylmethylene)hydrazine (BF26)

Light red powder, 97% yield; mp 235–236 °C; ^{1}H NMR (DMSO-d_6) δ 7.43 (s, 1H, C_5H-thiazole), 7.46–7.48 (m, 2H, Ar), 7.59–7.61 (m, 3H, naphthalene), 7.86–7.89 (m, 2H, Ar), 7.90–7.91 (m, 1H, naphthalene), 7.97–8.01 (m, 2H, naphthalene), 8.67 (s, 1H, =CH), 8.74–8.76 (m, 1H, naphthalene), 12.12 (br s, 1H, NH, D_2O exch.). Anal. Calcd for $C_{20}H_{14}ClN_3S$: C, 66.02; H, 3.88; N, 11.55. Found C, 66.38; H, 3.52; N, 11.79.

2.3.27. 1-(4-(4-Chlorophenyl)thiazol-2-yl)-2-(1-(naphthalen-2-yl)ethylidene)hydrazine (BF27)

Light yellow powder, 98% yield; mp 235–237 °C; ^{1}H NMR (DMSO-d_6) δ 2.45 (s, 3H, CH_3), 7.47 (s, 1H, C_5H-thiazole), 7.47–7.49 (m, 2H, Ar), 7.53–7.56 (m, 2H, naphthalene), 7.88–7.90 (m, 2H, Ar) 7.91–7.95 (m, 3H, naphthalene), 8.17–8.19 (m, 1H, naphthalene), 8.29–8.34 (m, 1H, naphthalene), 11.27 (br s, 1H, NH, D_2O exch.). Anal. Calcd for $C_{21}H_{16}ClN_3S$: C, 66.75%; H, 4.27%; N, 11.12%. Found C, 66.31; H, 4.59; N, 11.39.

2.3.28. 1-(4-(4-Chlorophenyl)thiazol-2-yl)-2-(1-(2H-chromen-2-oxo-3-yl)ethylidene)hydrazine (BF28)

Dark yellow powder, 98% yield; mp 243–244 °C; ^{1}H NMR (DMSO-d_6) δ 2.26 (s, 3H, CH_3), 7.42–7.45 (m, 3H, chromene), 7.46–7.48 (m, 2H, Ar), 7.53 (s, 1H, C_5H-thiazole), 7.82–7.85 (m,

1H, chromene), 7.87–7.89 (m, 2H, Ar), 8.16 (m, 1H, chromene), 11.75 (br s, 1H, NH, D_2O exch.). Anal. Calcd for $C_{20}H_{14}ClN_3O_2S$: C, 60.68; H, 3.56; N, 10.61. Found C, 60.99; H, 3.78; N, 10.98.

2.3.29. 9-(2-(4-(4-Chlorophenyl)thiazol-2-yl)hydrazono)-9H-fluorene-2-carboxylic acid (BF29)

Yellow powder, 93% yield; mp 190–191 °C; ^{1}H NMR (DMSO-d_6) δ 7.33 (s, 1H, C_5H-thiazole), 7.36–7.41 (m, 3H, fluorene), 7.48–7.50 (m, 2H, Ar), 7.74–7.79 (m, 2H, fluorene), 7.87–7.89 (m, 2H, Ar), 8.06–8.10 (m, 1H, fluorene), 8.33–8.38 (m, 1H, fluorene), 11.03 (s, 1H, NH, D_2O exch), 12.45 (br s, 1H, COOH, D_2O exch). Anal. Calcd for $C_{23}H_{14}ClN_3O_2S$: C, 63.96; H, 3.27; N, 9.73. Found C, 63.70; H, 3.50; N, 9.99.

2.3.30. 1-(4-(4-Chlorophenyl)thiazol-2-yl)-2-(1-(ferrocen-2-yl)ethylidene)hydrazine (BF30)

Brown powder, 89% yield; mp 220–221 °C; ^{1}H NMR (DMSO-d_6) δ 2.21 (s, 3H, CH_3), 4.17–4.21 (m, 5H, ferrocene), 4.38–4.40 (m, 2H, ferrocene), 4.62–4.65 (m, 2H, ferrocene), 7.33 (s, 1H, C_5H-thiazole), 7.44–7.46 (d, J = 8.0 Hz, 2H, Ar), 7.85–7.87 (d, J = 8.0 Hz, 2H, Ar), 11.08 (br s, 1H, NH, D_2O exch). Anal. Calcd for $C_{21}H_{20}ClFeN_3S$: C, 57.62; H, 4.60; N, 9.60. Found C, 57.99; H, 4.84; N, 9.98.

2.4. Yeast strains and growth

All yeast strains used in this study are listed in Table 1. The *gcn5*Δ, *elp3*Δ, and *sas2*Δ strains were produced in wild type S288c, whereas *rtt109*Δ in BY4742 genetic backgrounds. Yeast cells were grown at 28 °C in YPD medium (1% yeast extract, 2% bactopeptone, 2% glucose) liquid or solid (plus 2% agar). YPD was supplemented with solvent DMSO (1%). To test the sensitivity of the derivatives, 1 OD_{600}/mL of exponentially growing yeast cells were serially diluted (1/5) and spotted on solid medium containing each compound. All compounds were dissolved in DMSO and added to the medium at the indicated concentrations.

2.5. Histone bulk preparations and analysis

Yeast and human cell lines were lysed and total protein extracts were resuspended in 2× Laemli Buffer, boiled 10 min, loaded on 15% SDS–PAGE and blotted onto Hybond-C extra membranes (Amersham). Histones were detected with primary antibodies anti Ac-H3 (Millipore-06599), Ac-H4 (Millipore-06866), H3-AcK18 (Abcam-AB1191) and unmodified H3 (Millipore-06755). Signals were normalized with anti-Ada2 (Santa-Cruz SC6651) and anti-GAPDH (Glyceraldehyde 3-phosphate dehydrogenase, Santa-Cruz-SC32233). Proteins were detected by Enhanced Chemio-Luminescence (ECL) (Amersham) and visualized by film and ChemiDoc™ MP Imaging System (Biorad). Signals were quantified by Optiquant analysis software.

2.6. In vitro HAT assay

In vitro HAT assay was performed using 'HAT Assay Kit' (Active Motif). Briefly, HAT Buffer, specific recombinant HAT catalytic domain (80 ng, p300, Gcn5 or PCAF), 0.5 mM Acetyl-CoA and histone H3 (50 ng) were mixed and incubated at room temperature for 30 min, Developer and STOP solution were finally added. The assay is based on the response of a thiol-reactive fluorescent dye to the Co-A-SH generated by the histone acetyltransferase activity to give a fluorescent read-out.

Table 1
S. cerevisiae strains used in this work[28]

Strain	Genotype
S288c	*MAT alpha, SUC2, gal2, mal, mel, flo1 flo8-1, hap1*
*gcn5*Δ	*S288c background. Gcn5::KanMX*
*sas2*Δ	*S288c background. Sas2::KanMX*
*elp3*Δ	*S288c background. Elp3::KanMX*
BY4742	*MATa, his3-*Δ*1, leu2*Δ*, met15*Δ*, ura3*Δ
*gcn5*Δ	*BY4742 background, Gcn5::KanMX*
*rtt109*Δ	*BY4742 background, Rtt109::KanMX*

2.7. Assessment of cell viability

BF**1** was added at a final concentration of 50 and 100 μM, cells were collected and analyzed after incubation of 48/72 h at 37 °C. Cell viability of HeLa, U87 glioblastoma and BE-SK-N-BE(2) from ATCC (CRL2271) neuroblastoma cell lines was evaluated by trypan blue exclusion assay with respect to untreated controls.

3. Results

3.1. Yeast based screening for selective HAT inhibitors

In this study, the lead compound CPTH2 was used as the starting point for the targeted design and synthesis of a novel set of thiazole derivatives shown in Figure 1. In budding yeast, a strain carrying the deletion of two genes, which interact at the functional level, results in a sick phenotype and poor growth on plate. Similarly, a chemical compound may block the product of a gene that interacts with the query gene resulting in a sick phenotype (Fig. 2A). Overall, deletion of a non-essential query gene (Δ), that works together with the drug-target, causes hypersensitivity to sublethal drug concentrations and decreased growth. Therefore, compounds of BF series were tested in a yeast growth assay on wild type (WT) and an isogenic strain deleted in the HAT GCN5 (*gcn5*Δ) in order to identify molecules able to decrease the growth of the *gcn5*Δ strain on plate. Liquid cell cultures of wild type (S288c) and *gcn5*Δ strains were serially diluted, spotted on agar solid medium (YPD–DMSO 1%), and grown for 48 hours at 28 °C. The most active compounds BF**1**, BF**2**, and BF**3** (0.2 mM), identified in a previous screening, markedly reduced the growth of the *gcn5*Δ strain compared to CPTH2 (0.5 mM) and BF**19** (1 mM) chosen as an example of less active thiazole-based derivatives (Fig. 2B). The selectivity of compounds was then tested on other yeast strains deleted in different HATs such as Elp3 (*elp3*Δ), Sas2 (*sas2*Δ), and Rtt109 (*rtt109*Δ). The strains were spotted on plate and their growth was compared with the respective isogenic wild type: S288c and BY4742 (Fig. 3).

Previously characterized HAT inhibitors CPTH2 (0.5 mM) and curcumin (0.75 mM) were used as reference inhibitors (Fig. 3A). Results show that CPTH2 and curcumin inhibited *gcn5*Δ strain growth in both genetic backgrounds; they were instead ineffective on *elp3*Δ, *sas2*Δ, and *rtt109*Δ strains. The assay carried out with the synthesized derivatives demonstrated that among BF**1**, BF**2** and BF**3**, BF**1** was the most selective compound, able to inhibit almost exclusively the growth of *gcn5*Δ strain (Fig. 3B). Therefore, BF**1** was tested at different concentrations in budding yeast and it showed a dose-dependent inhibition with a significative effect at 0.1 mM (Fig. 3C). On the basis of these results, we focused on BF**1** compound for further analysis.

3.2. BF1 lowers global histone H3 acetylation in vivo and in vitro

We tested the ability of BF**1** to decrease global histone acetylation in the cell. Total protein extracts were analyzed and the global acetylation of histone H3 and H4 was tested by immunoblot (Fig. 4). Yeast cells treated with BF**1** (0.6 and 0.8 mM) and CPTH2 (0.8 mM), used as a control, were lysed and total extracts fractionated on PAGE.

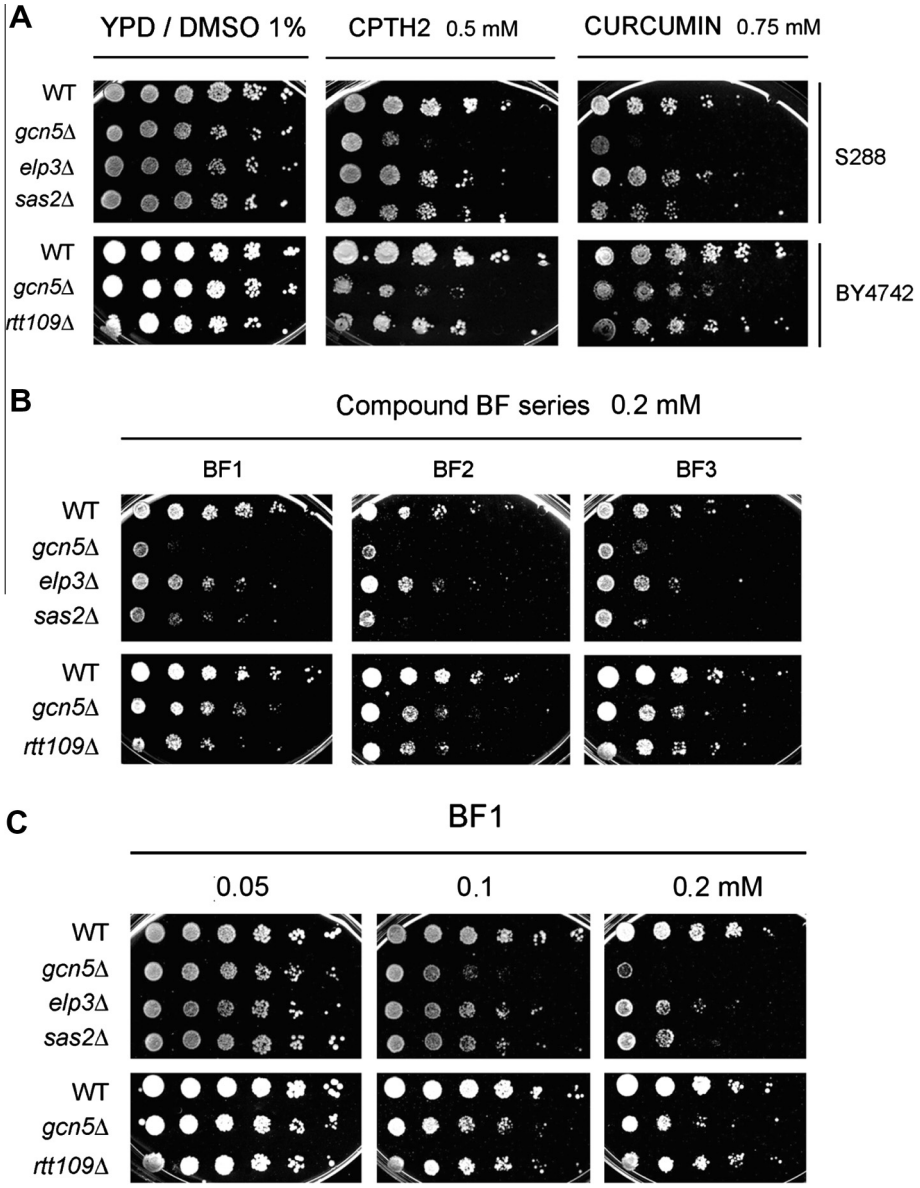

Figure 3. Growth inhibition tested on different HAT deleted strains. (A) Yeast growth assay was carried out on WT (S288c background) and isogenic strains deleted in HATs GCN5 (*gcn5*Δ), ELP3 (*elp3*Δ), SAS2 (*sas2*Δ), and on WT (BY4742 background) and isogenic GCN5 deleted (*gcn5*Δ) and RTT109 deleted (*rtt109*Δ) strains. Cells were serially diluted and spotted on YPD–DMSO 1%, CPTH2 (0.5 mM) and curcumin (0.75 mM) used as reference inhibitors. (B) Compounds BF**1**, BF**2**, and BF**3** (0.2 mM) tested on indicated HAT deleted strains. (C) Gcn5 selective inhibitor BF**1** tested at increasing concentrations (0.05, 0.1 and 0.2 mM) showed to preferentially inhibit the *gcn5*Δ strain.

Immunoblot was probed for acetylated histone H3 (Ac-H3) and H4 (Ac-H4), unmodified histone H3 (H3) and constitutively expressed ADA2 protein (Fig. 4A). Results were quantified, normalized and levels of histone AcH3 and AcH4 with respect to untreated controls (C) were reported (Fig. 4B). BF**1** treated cells showed a 50% decrease in histone H3 acetylation, whereas the level of histone H4 acetylation was not affected, indicating histone H3 substrate selectivity. Based on these results, we tested if BF**1** was also able to inhibit the catalytic HAT reaction: this was evaluated in order to assess the specificity of BF**1** and avoid more indirect effects. Fluorescent HAT in vitro assay was used and human recombinant p300, Gcn5 and PCAF were tested on histone H3. Untreated samples were taken as control (C) and HATs inhibition was measured by determination of residual enzyme activity in presence of the inhibitor. PCAF was tested but its catalytic activity was not inhibited by BF**1** treatment (data not shown). The results were diagrammed in Figure 5. The reaction catalyzed by Gcn5 (Fig. 5A) was no significatively reduced, while that catalyzed by p300 (Fig. 5B) was almost abolished by BF**1** (0.6 mM) with respect to untreated control and is fully comparable to anacardic acid, used as reference inhibitor. Overall, the measured inhibitory activity revealed that BF**1** not only had effect on functional interacting partners of Gcn5, but showed a preferential effect on p300 in vitro. These results suggest that the yeast approach may represent a preliminary convenient step to screen a large number of compounds, although further in vitro inhibitory activity characterization of the most active derivatives is required.

3.3. BF1 affects histone H3 acetylation in human cancer cell lines

Next we wanted to evaluate the effect of BF**1** on human cell lines. HeLa cells were used as a widely accepted control line. Two different cell lines derived from aggressive tumours: U87,

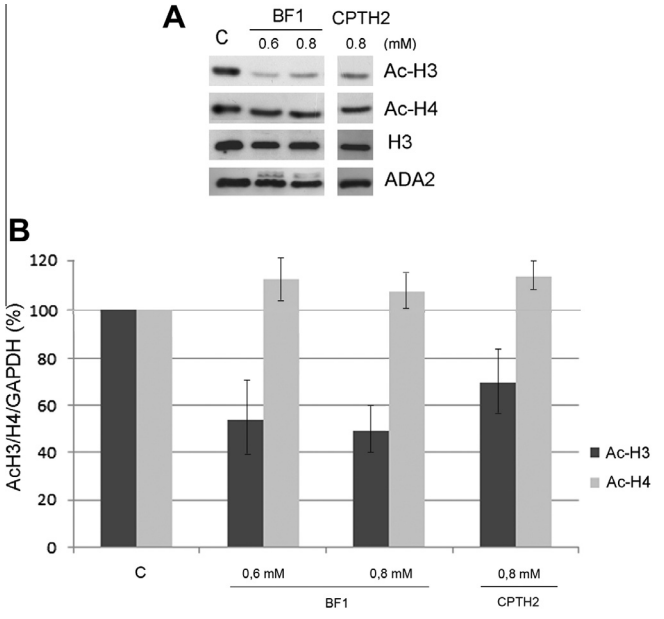

Figure 4. BF1 inhibits acetylation of histone H3 at global level. (A) Acetylation of bulk histones H3 and H4 was investigated by Western blot. Wild type yeast cells (S288c) were grown in rich medium YPD–DMSO 1% (C), supplemented with BF**1** (0.6 and 0.8 mM) or with lead compound CPTH2 (0.8 mM). Total proteins extracts were run on PAGE and hybridized with antibody against panacetylated histones (Ac-H3 and Ac-H4), unmodified histone H3 and constitutively expressed ADA2 protein, both used as internal loading standards. (B) Histograms report global histone H3 (black bar) and H4 (grey bar) acetylation percentage observed in absence (C) or in presence of BF**1** (0.6 and 0.8 mM) and CPTH2 (0.8 mM). Each value was normalized to the internal amount of constitutively expressed ADA2. The error bars represent the standard deviation from experiments performed in triplicate.

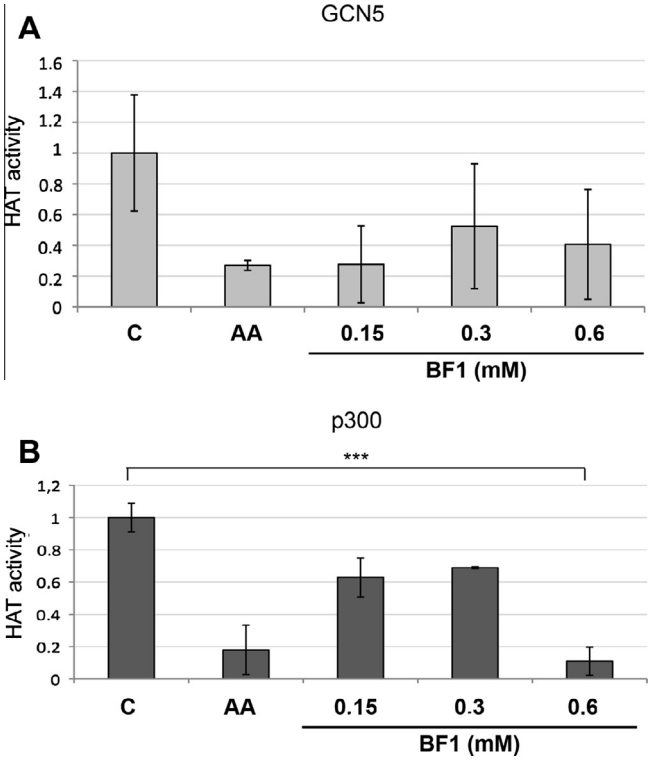

Figure 5. BF**1** inhibition of in vitro histone H3 acetylation by recombinant Gcn5 and p300. (A) Recombinant Gcn5 was assayed in the presence of acetyl-CoA and histone H3 substrate. Reaction was performed without inhibitor (C), in the presence of anacardic acid, AA (15 μM) as reference inhibitor and at increasing BF**1** concentrations (0.15, 0.3 and 0.6 mM). (B) Recombinant p300 was tested in the same conditions of Gcn5. Each reaction was repeated three times. Standard errors are shown and $p = 0.0003$.

glioblastoma and BE, neuroblastoma were tested in parallel. Cells were incubated for 24 (not shown), 48 and 72 h in presence of BF**1** at two different concentrations, 50 and 100 μM. BF**1** concentrations used on cell cultures were sensibly lower than in yeast where the cell wall requires higher concentrations of compounds to obtain an efficient cellular uptake. The decrease of both, bulk acetylation of histone H3 (Ac-H3) and acetylation of lysine K18 (H3-AcK18), which has been indicated as a promising prognostic mark for a number of tumours,[36] was evaluated. Cells were lysed and total protein extracts analyzed. Figure 6 (Panel A) shows western blot analysis of total protein extracts of respectively HeLa, U87 glioblastoma, and BE neuroblastoma cell lines. Levels of respectively, panacetylated Ac-H3 and H3-AcK18 were normalized to GAPDH, used as uniformly expressed protein internal loading control. Collected results are diagrammed in the histograms of Figure 6 (Panels B and C). Although the drug response is variable, all the tested cell lines showed a concentration-dependent decrease of acetylation and after 72 h incubation with BF**1** at 100 μM, both AcH3 and H3-AcK18 were drastically and almost completely reduced. However, in this figure, 72 h treatment was not statistically analyzed in detail because of unwanted side effects due to prolonged drug treatment. Noteworthy, BF**1** inhibited histone H3 acetylation without affecting the expression of constitutive GAPDH.

Having corroborated the inhibitory effect of BF**1** on histone H3 acetylation, we evaluated the viability of cells exposed to the same BF**1** treatment (Fig. 6 Panel D). As shown, cell viability in HeLa and glioblastoma U87 cell lines was only slightly affected by BF**1** administration. In neuroblastoma BE cells, a decrease (~30%) in cell viability, compared to the control, was observed after 72 h treatment (BF**1** at 100 μM). Collectively, these results show that BF**1** is able to inhibit histone H3 acetylation in human cell lines and, in particular, in derived tumours glioblastoma and neuroblastoma. The cell viability was not much affected during BF**1** treatment indicating a low toxicity of BF**1** on human cells.

4. Discussion

A major challenge in drug discovery is to identify the proteins and cellular pathways affected by a new drug. On the basis of the biological activity recorded for a large series of derivatives of previously described HAT inhibitor CPTH2,[28] we can describe the general features of the structural requirements that lead to a novel group of HAT inhibitors named BF. Our analysis indicates that the 4-chlorophenyl moiety in the C4 position of the thiazole nucleus seems to be preferred. Furthermore, chemical changes of the hydrazonic nitrogen in C2 suggested that both, the cyclopentane ring modification (compounds BF**10**–BF**12**) and/or the aromatization/complication (compounds BF**13**–BF**30**) reduce the biological activity (*i.e.*, BF**19** in Fig. 2B). On the opposite, better results were obtained by ring opening and chain shortening, thus correlating the inhibitory strength to a limited steric hindrance in this portion of the pharmacophore (compounds BF**1**–BF**9**). The best data were registered with the smallest derivatives of the series (BF**1**–BF**3**), where the cyclopentane skeleton of the lead compound CPTH2 was simplified. Our collected results indicate that BF**1** represents a novel HAT inhibitor and, by means of yeast based genetic assay, this test compound is shown to interfere with a functional counterpart of Gcn5. In fact, similarly to the double deletion genetically obtained of two interacting genes, BF**1** is able to affect one component required by Gcn5 at functional level.

This pre-screening offers a simple approach and represents a convenient tool for the biological evaluation of new compounds.[37]

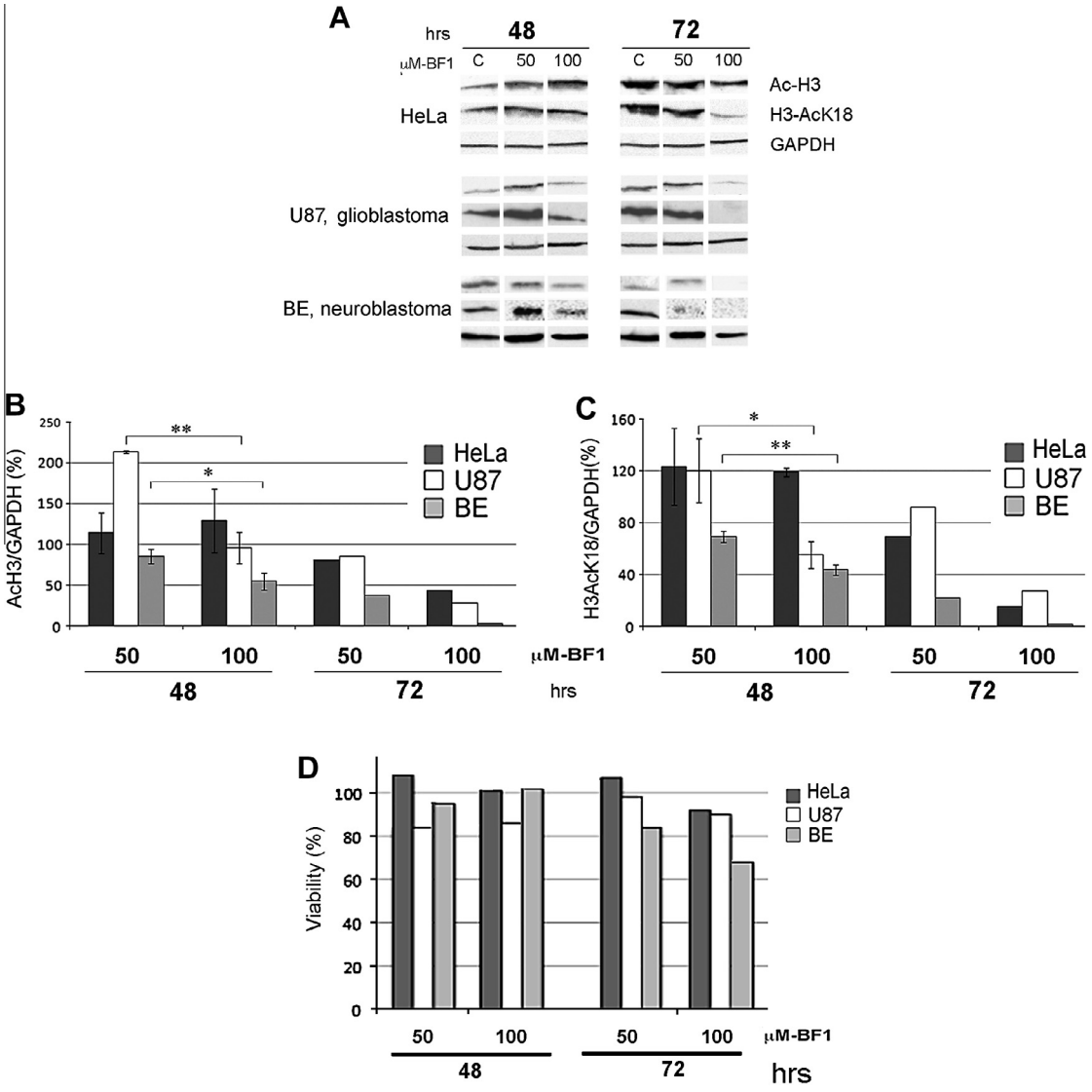

Figure 6. BF**1** is a p300/Gcn5 inhibitor and reduces acetylation of histone H3 and H3K18 in human cell lines. Panel (A) Western blot analysis of histone H3, panacetylated (AcH3), acetylated at Lys-18 (H3AcK18) and GAPDH as internal loading control. HeLa, U87-glioblastoma, and BE-neuroblastoma cell lines were grown for 48 and 72 h without (C) or in presence of BF**1** (50 and 100 μM). Histograms show the percentage of AcH3 (Panel B) and H3AcK18 (Panel C) normalized to the constitutively expressed GAPDH in HeLa (dark grey bar), U87 (white bar), and BE (light grey bar) cells. Each experiment represents the average of three different biological replicates, unless otherwise stated. Standard errors are shown and asterisks are as follows: $^{**}p$ <0.001 and $^{*}p$ <0.05. (Panel D) viability of indicated cell lines treated with BF**1** (50 and 100 μM) for 48 and 72 h. On the average, 1.5×10^5 cells were counted for each point. Viability was expressed as the mean percentage of viable/dead cells with respect to the untreated control.

On the basis of highly conserved HAT catalytic domain in evolution, the identification of an inhibitory activity selective for GCN5 established in yeast may further justify a similar biological effect on other HATs such as p300 working in human cells. In addition, it was recently reported that a single inhibitor may show activity towards multiple HATs such as p300, CBP and GCN5.[19b] Similarly, CPTH2, the lead compound of BF**1,** firstly identified in yeast,[28] was successfully employed as potent inhibitor of GCN5 and PCAF, confirming its role on epigenetic regulation.[29]

Here we report the identification of a biologically active molecule, BF**1**, that was further validated in vivo, in yeast and human cell cultures, and in vitro.

A selective inhibition of histone H3 acetylation as well as an increased level of AcH4 were observed by BF**1** treatment: this result fits to a previous report showing that bulk hyperacetylation of histone H4 is simultaneously found with H3 hypoacetylation.[38] BF**1** inhibitory activity was next tested by in vitro HAT assay (with Gcn5, p300 and PCAF): this experiment was performed to rule out an indirect effect of this proposed lead compound. BF**1** showed to be able to lower the catalytic activity of recombinant Gcn5 and mainly p300, thus providing direct evidence for its efficacy on the acetylation reaction itself. In vitro, the inhibition on p300 was higher than the inhibition on Gcn5, whereas no effect on PCAF was observed, highlighting the selective inhibition of BF**1** toward different HATs. The higher activity found on p300 is not surprising since we used the yeast approach only to narrow the search for active compounds. In budding yeast p300 is not present; therefore it is likely that BF**1** may show a higher selectivity for p300. To gain insights on BF**1** efficacy on human cell lines, we decided to analyze the histone H3 acetylation in two aggressive tumour derived cell lines, glioblastoma-U87 and neuroblastoma-BE. HeLa was used as a *bona fide* reference cell line, not derived from brain. We measured the acetylation status of both global histone H3 and its specific lysine 18 (H3AcK18) because it was demonstrated to be a valuable prognostic indicator in several human cancers.[36] BF**1** showed to be active on human cell lines and after 72 h of treatment, the global level of AcH3 and H3AcK18 was drastically reduced.

Collectively, our results describe the synthesis, identification, and characterization of a novel HAT inhibitor, BF**1**, which was shown in vitro to be mainly active on p300. Furthermore, BF**1** proved to lower in vivo the global acetylation of histone H3 (AcH3 and H3AcK18) in yeast and in human cell lines. Moreover, it is known that acetylation targets not only histones but also non-histone factors, such as transcription activators. Accordingly, the induction of oncogenes or aberrant gene activation like in cardiomyocyte hypertrophy[39] or on HIV replication cycle[40] may be profitably investigated with selective HAT inhibitors, which are far less studied with respect to the widely described HDACs inhibitors. For all these reasons, we believe that the identification and characterization of novel HAT inhibitors will open the way to novel applications in basic research and in therapy.

Acknowledgments

This work was supported by PRIN 2009 (Prot. 200973ST5Y_002), FIRB; Fondazione Cenci-Bolognetti, and Filas (ASR2, Regione Lazio, Italy). We thank contribution and technical skill of M. Marchioni, IBPM-CNR, for experiments on human cell cultures.

References and notes

1. Li, G.; Reinberg, D. *Curr. Opin. Genet. Dev.* **2011**, *21*, 175.
2. Caffarelli, E.; Filetici, P. *Front. Biosci.* **2011**, *17*, 2682.
3. Marks, P. A.; Richon, V. M.; Miller, T.; Kelly, W. K. *Adv. Cancer Res.* **2004**, *91*, 137.
4. Adachi, M.; Zhang, Y.; Zhao, X.; Minami, T.; Kawamura, R.; Hinoda, Y.; Imai, K. *Clin. Cancer Res.* **2004**, *10*, 3853.
5. Park, S. Y.; Jun, J. A.; Jeong, K. J.; Heo, H. J.; Sohn, J. S.; Lee, H. Y.; Park, C. G.; Kang, L. *Oncol. Rep.* **2011**, *25*, 1677.
6. Furdas, S. D.; Kannan, S.; Sippl, W.; Jung, M. *Arch. Pharm. Chem. Life Sci.* **2012**, *345*, 7.
7. Singh, S.; Khar, A. *Anticancer Agents Med. Chem.* **2006**, *6*, 259.
8. Capaccione, K. M.; Pine, S. R. *Carcinogenesis* **2013**, *34*, 1420.
9. Lee, H.; Zhang, P.; Herrmann, A.; Yang, C.; Xin, H.; Wang, Z.; Hoon, D. S.; Forman, S. J.; Jove, R.; Riggs, A. D.; Yu, H. *Proc. Natl. Acad. Sci. U.S.A.* **2012**, *109*, 7765.
10. Heemers, H. V.; Sebo, T. J.; Debes, J. D.; Regan, K. M.; Raclaw, K. A.; Murphy, L. M.; Hobisch, A.; Culig, Z.; Tindall, D. J. *Cancer Res.* **2007**, *67*, 3422.
11. Atadja, P. W. *Prog. Drug Res.* **2011**, *67*, 175.
12. Vernarecci, S.; Tosi, F.; Filetici, P. *Epigenetics* **2010**, *5*, 105.
13. Dekker, F. J.; Haisma, H. J. *Drug Discovery Today* **2009**, *14*, 942.
14. Balasubramanyam, K.; Varier, R. A.; Altaf, M.; Swaminathan, V.; Siddappa, N. B.; Ranga, U.; Kundu, T. K. *J. Biol. Chem.* **2004**, *279*, 51163.
15. Balasubramanyam, K.; Swaminathan, V.; Ranganathan, A.; Kundu, T. K. *J. Biol. Chem.* **2003**, *278*, 19134.
16. Mantelingu, K.; Reddy, B. A.; Swaminathan, V.; Kishore, A. H.; Siddappa, N. B.; Kumar, G. V.; Nagashankar, G.; Natesh, N.; Roy, S.; Sadhale, P. P.; Ranga, U.; Narayana, C.; Kundu, T. K. *Chem. Biol.* **2007**, *14*, 645.
17. Choi, K. C.; Jung, M. G.; Lee, Y. H.; Yoon, J. C.; Kwon, S. H.; Kang, H. B.; Kim, M. J.; Cha, J. H.; Kim, Y. J.; Jun, W. J.; Lee, J. M.; Yoon, H. G. *Cancer Res.* **2009**, *69*, 583.
18. Ravindra, K. C.; Selvi, B. R.; Arif, M.; Reddy, B. A.; Thanuja, G. R.; Agrawal, S.; Pradhan, S. K.; Nagashayana, N.; Dasgupta, D.; Kundu, T. K. *J. Biol. Chem.* **2009**, *284*, 24453.
19. (a) Bowers, E. M.; Yan, G.; Mukherjee, C.; Orry, A.; Wang, L.; Holbert, M. A.; Crump, N. T.; Hazzalin, C. A.; Liszczak, G.; Yuan, H.; Larocca, C.; Saldanha, S. A.; Abagyan, R.; Sun, Y.; Meyers, D. J.; Marmorstein, R.; Mahadevan, L. C.; Alani, R. M.; Cole, P. A. *Chem. Biol.* **2010**, *17*, 471; (b) Yang, H.; Pinello, C. E.; Luo, J.; Li, D.; Wang, Y.; Zhao, L. Y.; Jahn, S. C.; Saldanha, S. A.; Planck, J.; Geary, K. R.; Ma, H.; Law, B. K.; Roush, W. R.; Hodder, P.; Liao, D. *Mol. Cancer Ther.* **2013**, *2*, 610.
20. Lau, O. D.; Kundu, T. K.; Soccio, R. E.; Ait-Si-Ali, S.; Khalil, E. M.; Vassilev, A.; Wolffe, A. P.; Nakatani, Y.; Roeder, R. G.; Cole, P. A. *Mol. Cell* **2000**, *5*, 589.
21. Biel, M.; Kretsovali, A.; Karatzali, E.; Papamatheakis, J.; Giannis, A. *Angew. Chem., Int. Ed.* **2004**, *43*, 3974.
22. Stimson, L.; Rowlands, M. G.; Newbatt, Y. M.; Smith, N. F.; Raynaud, F. I.; Rogers, P.; Bavetsias, V.; Gorsuch, S.; Jarman, M.; Bannister, A.; Kouzarides, T.; McDonald, E.; Workman, P.; Aherne, G. W. *Mol. Cancer Ther.* **2005**, *4*, 1521.
23. Dekker, F. J.; Ghizzoni, M.; van der Meer, N.; Wisastra, R.; Haisma, H. J. *Bioorg. Med. Chem.* **2009**, *17*, 460.
24. Ghizzoni, M.; Haisma, H. J.; Dekker, F. J. *Eur. J. Med. Chem.* **2009**, *44*, 4855.
25. Wisastra, R.; Ghizzoni, M.; Maarsingh, H.; Minnaard, A. J.; Haisma, H. J.; Dekker, F. J. *Org. Biomol. Chem.* **2011**, *9*, 1817.
26. Mai, A.; Rotili, D.; Tarantino, D.; Nebbioso, A.; Castellano, S.; Sbardella, G.; Tini, M.; Altucci, L. *Bioorg. Med. Chem. Lett.* **2009**, *19*, 1132.
27. Mai, A.; Rotili, D.; Tarantino, D.; Ornaghi, P.; Tosi, F.; Vicidomini, C.; Sbardella, G.; Nebbioso, A.; Miceli, M.; Altucci, L.; Filetici, P. *J. Med. Chem.* **2006**, *49*, 6897.
28. Chimenti, F.; Bizzarri, B.; Maccioni, E.; Secci, D.; Bolasco, A.; Chimenti, P.; Fioravanti, R.; Granese, A.; Carradori, S.; Tosi, F.; Ballario, P.; Vernarecci, S.; Filetici, P. *J. Med. Chem.* **2009**, *52*, 530.
29. (a) Kikuchi, H.; Kuribayashi, F.; Kiwaki, N.; Takami, Y.; Nakayama, T. *J. Immunol.* **2011**, *186*, 3015; (b) Li, G.; White, C. A.; Lam, T.; Pone, E. J.; Tran, D. C.; Hayama, K. L.; Zan, H.; Xu, Z.; Casali, P. *Cell Rep.* **2013**, *5*, 702; (c) Ablack, J. N. G.; Cohen, M.; Thillainadesan, G.; Fonseca, G. J.; Pelka, P.; Torchia, J.; Mymryk, J. S. *J. Virol.* **2012**, *86*, 8198.
30. Matsumoto, T.; Yun, C. S.; Yoshikawa, H.; Nishida, H. *PLoS ONE* **2011**, *6*, e16372.
31. Zou, Y.; Bi, X. *Nucleic Acids Res.* **2008**, *36*, 5189.
32. Kolonko, E. M.; Albaugh, B. N.; Lindner, S. E.; Chen, Y.; Satyshur, K. A.; Arnold, K. M.; Kaufman, P. D.; Keck, J. L.; Denu, J. M. *Proc. Natl. Acad. Sci. U.S.A.* **2010**, *107*, 20275.
33. Ruotolo, R.; Tosi, F.; Vernarecci, S.; Ballario, P.; Mai, A.; Filetici, P.; Ottonello, S. *Genomics* **2010**, *96*, 272.
34. (a) Chimenti, F.; Secci, D.; Bolasco, A.; Chimenti, P.; Granese, A.; Carradori, S.; Yáñez, M.; Orallo, F.; Sanna, M. L.; Gallinella, B.; Cirilli, R. *J. Med. Chem.* **2010**, *53*, 6516; (b) Carradori, S.; D'Ascenzio, M.; De Monte, C.; Secci, D.; Yáñez, M. *Arch. Pharm.* **2013**, *346*, 17.
35. (a) Cirilli, R.; Ferretti, R.; La Torre, F.; Secci, D.; Bolasco, A.; Carradori, S.; Pierini, M. *J. Chromatogr. A* **2007**, *1172*, 160; (b) Carradori, S.; Cirilli, R.; Dei Cicchi, S.; Ferretti, R.; Menta, S.; Pierini, M.; Secci, D. *J. Chromatogr. A* **2012**, *1269*, 168.
36. Hoseok, I.; Ko, E.; Kim, Y.; Cho, E. Y.; Han, J.; Park, J.; Kim, K.; Kim, D. H.; Shim, Y. M. *Cancer Epidemiol. Biomarkers Prev.* **2010**, *19*, 566.
37. Menacho-Marquez, M.; Murguia, J. R. *Clin. Trans. Oncol.* **2007**, *9*, 221.
38. Agricola, E.; Verdone, L.; Di Mauro, E.; Caserta, M. *Mol. Microbiol.* **2006**, *62*, 1433.
39. Morimoto, T.; Sunagawa, Y.; Fujita, M.; Hasegawa, K. *Circ. J.* **2010**, *74*, 1059.
40. Terreni, M.; Valentini, P.; Liverani, V.; Gutierrez, M. I.; Di Primio, C.; Di Fenza, A.; Tozzini, V.; Allouch, A.; Albanese, A.; Giacca, M.; Cereseto, A. *Retrovirology* **2010**, *7*, 18.